JACS
JOURNAL OF THE AMERICAN CHEMICAL SOCIETY

Communication

pubs.acs.org/JACS

Controlled Interconversion of Superposed-Bistriangle, Octahedron, and Cuboctahedron Cages Constructed Using a Single, Terpyridinyl-Based Polyligand and Zn^{2+}

Ting-Zheng Xie,[†] Kevin J. Endres,[‡] Zaihong Guo,[‡] James M. Ludlow III,[†] Charles N. Moorefield,[†] Mary Jane Saunders,[§] Chrys Wesdemiotis,*[,†,‡] and George R. Newkome*[,†,‡]

[†]Departments of Polymer Science and [‡]Chemistry, The University of Akron, Akron, Ohio 44325, United States

[§]Department of Biological Sciences, Florida Atlantic University, Boca Raton, Florida 33431, United States

Supporting Information

ABSTRACT: Metallomacromolecular architectural conversion is expanded by the characterization of three different structures. A quantitative, single-step, self-assembly of a shape-persistent monomer, containing a flexible crown ether moiety, gives an initial Archimedean-based cuboctahedron that has been unequivocally characterized by 1D and 2D NMR spectroscopy, mass spectrometry, and collision cross section analysis. Both dilution and exchange of counterions, transforms this cuboctahedron into two identical octahedrons, which upon further dilution convert into four, superposed, *bis*trianglar complexes; increasing the concentration reverses the process. Ion binding studies using the cuboctahedral cage were undertaken.

Within the biological realm, molecular folding, structural rearrangement, and subunit association play important roles in catalysis and biological processes.[1−3] An example of molecular architectural rearrangement, reminiscent of microbial fission and fusion process, has been described.[4] Considering these phenomena, supramolecular capsules,[5] grippers,[6] and cages,[7,8] wherein conformation can be tuned by ionic and environmental stimuli have been reported. Notably, the construction of molecular devices in many cases relies on an assembly-disassembly-reassembly process wherein the overall architecture of the original construct is maintained.[9,10]

Coordination-driven self-assembly provides a powerful tool to access polyhedral supramolecules[11] such as the tetrahedron,[12] octahedron,[13] rhombicuboctahedron,[14] and dodecahedron[15,16] due in part, to ligand−metal directivity and shape-persistent frameworks. Utilizing terpyridine-based monomers that coordinate with transition metal ions [i.e., ⟨tpy-M^{2+}-tpy⟩ (M = transition metal ion)] as the linkage units, we have reported numerous self-assembled supramolecules including triangles,[17] hexagons,[18] Sierpiński triangle,[19,20] and various spoked wheels.[21,22] Most recently, we also transformed from one motif to another by simply changing the concentration or the counterions. Herein we expand on this fission−fusion process.[4] Thus, the design and synthesis of a novel, flexible, X-shaped, tetra*kis*terpyridinyl ligand **3** that can easily adopt 127°, 90°, and 0° dihedral angles to generate the corresponding supramolecular cages with cuboctahedral, octahedral, and superposed[23] *bis*trianglar architectures (i.e., **4**−**6**), respectively. Thus, self-assembly of polyligand **3** with Zn^{2+} ions can be controlled by concentration and counterions to give exclusively the desired motif or mixtures of each. (Scheme 1).

Scheme 1. Preparation of the Zn^{2+}-Based, Cuboctahedron (4), Octahedron (5), and Superposed *Bis*triangle (6) and the Monomer's Initial Conformations

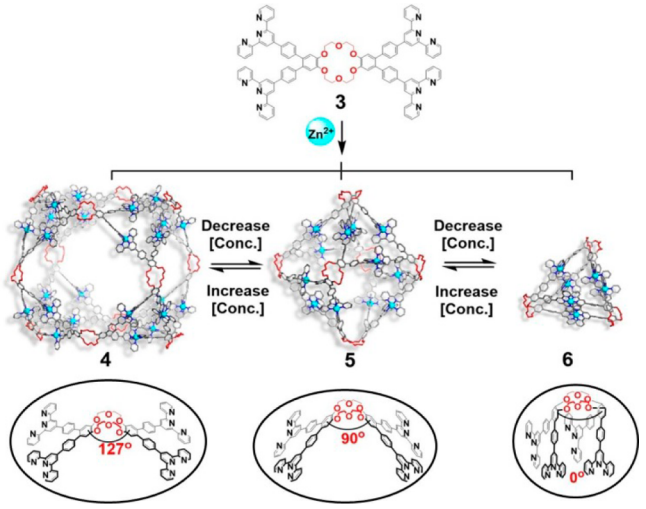

Ligand **3** possesses an 18-crown-6 moiety that connects two 60°-based, *bis*terpyridinyl-substituted benzene rings, which, in the presence of stimuli,[24] can freely fold or unfold in the range of 0° to 180°. Preparation of the ligand **3** was accomplished by treatment of 2,3,13,14-tetrabromodibenzo-18-crown-6[25] (**1**) with four equivalents of 4-(2,2′:6′,2″-terpyridinyl)-phenylboronic acid (**2**)[26] gave the desired tetra*kis*ligand. The ^{1}H NMR spectrum of **3** exhibited a sole set of signals attributed to the terpyridinyl moieties suggesting free rotation throughout the two sets of 60° juxtaposed arms, along with a singlet at 7.07 ppm assigned to the aryl protons of the dibenzo-18-crown-6 moiety. Two triplets appearing at 4.36 and 4.14 ppm were assigned to the crown ether methylene groups (see Figure 3a).

Received: August 1, 2016
Published: September 9, 2016

ACS Publications © 2016 American Chemical Society

DOI: 10.1021/jacs.6b07969
J. Am. Chem. Soc. 2016, 138, 12344−12347

The one-step, self-assembly of ligand **3** using a precise ratio (1:2) of $Zn(NO_3)_2$ in a stirred mixture of MeOH and $CHCl_3$ (1:1, v/v) at 25 °C for 1 h led to a clear pale-yellow solution, which, based on preliminary NMR data, gave (>98%) the desired **4**, as a light-yellow precipitate. Anion exchange was conducted to modify solubility of the product(s) in different solvents; thus, treatment with either saturated aqueous NH_4PF_6 or $NaBPh_4$ gave the PF_6^- or BPh_4^- salts, respectively. The core 18-crown-6 moiety adapts readily to allow the two, opposed, 60°-oriented, *bis*terpyridinyl units to conform to the 127° dihedral angle, as expected.

In comparison to our previously reported cuboctahedron possessing a rigid anthracene-based building block,[4] this cuboctahedron upon dilution gave the octahedral-shaped cage **5**, formed by combining 6 "X"-shaped ligands **3** and 12 zinc ions. Upon further dilution, or notably, counterion change from PF_6^- to BPh_4^-, 2 equiv of the *bis*triangular cage **6** were generated with 3 "X"-shaped ligands **3** and 6 metal ions; the process was observed and confirmed to be reversible by mass spectroscopy and NMR. For this unique phenomenon, the observed ratio of **4**:**5**:**6** upon successive dilutions is 1:2:4, respectively[4,27] (Le Chatelier's principle).

The ESI-MS (electrospray ionization-mass spectroscopy) spectrum of **4** with 48 PF_6^- anions (Figure 1) in a solution of

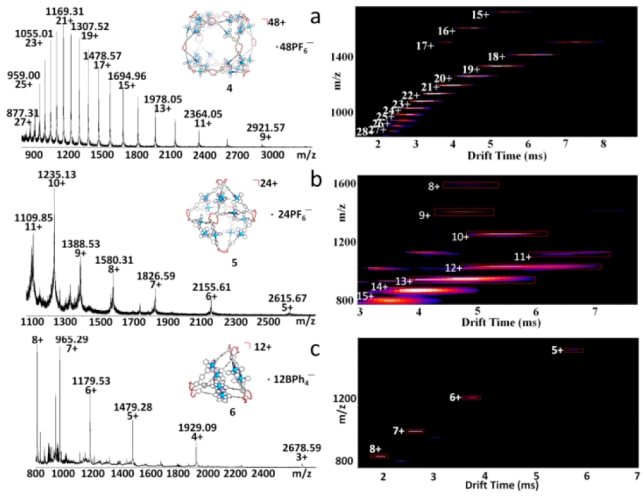

Figure 1. ESI- and TWIM-MS spectra: (a) cuboctahedron **4**·48 PF_6^- in DMSO and MeCN (v/v 1:10; 0.5 mg/mL); (b) octahedron **5**·24 PF_6^- in DMSO and MeCN (v/v 1:10; 0.2 mg/mL); (c) *bis*triangle **6**·12 BPh_4^- in DMSO and MeCN (v/v 1:100; 5 μg/mL).

MeCN and DMSO (500 μg/mL) confirms the cuboctahedron shape by revealing a series of dominant peaks corresponding to charge states ranging from 24+ to 8+ (Figure S15). These MS results provide strong support for a combination of 12 ligands (i.e., **3**) and 24 Zn^{2+} ions, along with the theoretical *m*/*z* values for each charge state, and are consistent with the corresponding calculated values. Notably, dilution of this solution of **4** to 0.05 mg/mL with MeCN or MeCN and DMSO (0.2 mg/mL), led to an ESI-MS spectrum showing intense signals at 1109.9, 1235.1, 1388.5, 1580.3, 1826.6, 2155.6, and 2615.7 *m*/*z*, corresponding to charge states 11+ to 5+, respectively. This confirmed the structural transformation to a different complex **5** with a combination of 6 ligands and 12 Zn^{2+} metal ions, which supports an octahedron-shaped structure. Still further dilution or changing the counterions to BPh_4^- gave the *bis*trianglar complex **6** that was also characterized by ESI-MS, thereby providing strong evidence for the combination of 3 ligands and 6 Zn^{2+} ions. The observed isotopic distribution pattern for the 7+ species for structure **6** corresponds well with the simulated pattern (Figure S12).

Additional support (Figures 1, S16) for **4** was provided by ESI-TWIM-MS experiments[27,28] to resolve isomeric ions and determine structural information that serves as a unique complement to the more traditional characterization procedures.[29−31] The TWIM-MS spectrum of complex **4** exhibits charge states ranging from 25+ to 18+, derived from **4** with a narrow band for each charge state and a narrow drift time distribution for the signals extracted for each band, indicative of a single species; this is consistent with the ESI results. The TWIM-MS image suggests a slight conformational change at different charge states. From charge states of 17+ to 13+, the drift time shows a short shift when compared with the charge states from 25+ to 18+, and as the charge states go above 13+, the drift time becomes much shorter. This phenomenon suggests that when there are more anions on a spherical complex with positive charge, it gives a more compact conformation, and when there is a more positive charge on the complex with more electrostatic repulsion, it gives a more open overall conformation.

The ESI-MS spectrum of a mixture of cages **4**−**6** reveals specific charged species that can be directly assigned to cuboctahedron **4** and *bis*triangle **6** (Figure 2); peaks calculated

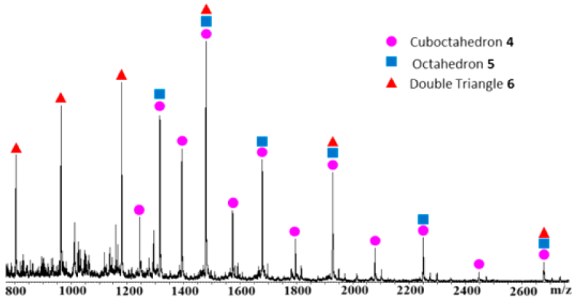

Figure 2. ESI-MS of a mixture of **4**, **5**, and **6** with peaks labeled corresponding to the calculated charged fragments for each cage.

for octahedron **5** overlapped with **4** and **6**, as expected. This overlap gives higher peaks due to an increased amount of identical charged species originating from the different cages.

The ^{1}H NMR spectrum of **4** (in DMSO-d_6) exhibited a single set of peaks indicating the formation of a single, highly symmetric species where all identically positioned nuclei are chemically and magnetically equivalent (Figure 3b). COSY and NOESY NMR experiments were used to verify the assignments of the ^{1}H NMR spectra. Comparison of the ^{1}H NMR spectrum of ligand **3** with that of **4** shows that the signals of each methylene group are split into two groups; the peak at 4.32 ppm for **3** is split into two signals at 4.40 and 4.00 ppm for **4**. The dibenzo crown ether adopts a stable *cis* conformation upon complexation, in which the methylene groups have two different environments. The expected upfield shift of the 6,6″-tpy*H* doublet from 8.68 to 7.94 ppm is attributed to the ⟨tpy-Zn^{2+}-tpy⟩ connectivity. All other signals show the characteristic downfield shifts following complex formation. In the spectrum of octahedron **5** (Figure 3c), there is also a single set of peaks indicative of a highly symmetric complex. When compared with the cuboctahedron **4**, all the peaks for **5** show an upfield shift, which suggests that the formation of a

DOI: 10.1021/jacs.6b07969
J. Am. Chem. Soc. 2016, 138, 12344−12347

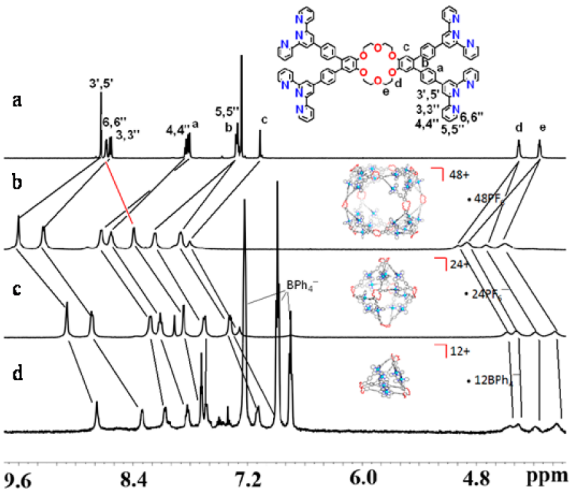

Figure 3. ^{1}H NMR spectra of (a) ligand **3** in $CDCl_3$; (b) cuboctahedron **4**·48 PF_6^- in DMSO-d_6 (1.0 mg/mL); (c) octahedron **5**·24 PF_6^- in DMSO-d_6 and CD_3CN (v/v 1:10; 0.2 mg/mL); (d) superposed-*bis*triangle **6**·12 BPh_4^- in DMSO-d_6 and CD_3CN (v/v 1:100; 5 μg/mL).

smaller structure with similar components.[4] The ^{1}H NMR spectrum (Figure 3d) of *bis*triangular complex **6** was obtained by dilution of the cuboctahedron with BPh_4^- counterions, which showed an enhanced upfield shift when compared with the spectra of the other two larger structures. Notably, a variable temperature ^{1}H NMR experiment (Figure S8) performed from −10 to +50 °C in the concentration 0.4 mg/mL for complexes **4** and **5** suggests a dynamic equilibrium exists between the two species.

The ^{1}H 2D DOSY NMR spectrum of complex **4** (Figure S6) clearly shows a single band with a diffusion coefficient D = 10^{-10}, along with a corresponding solvent band (log D = −9.14), indicative of a single species in DMSO-d_6. The calculated diameter of the spherical complex, based on the viscosity of DMSO-d_6 at 298 K (2.0×10^{-3} N m^{-2} s), is 6.06 nm; DOSY experiments for octahedron **5** and *bis*triangle **6** were performed (Figure S7) and the diameters of **5** and **6** were determined to be 4 and 2.8 nm, respectively. These results are consistent with the modeling data.

Further evidence includes the collision cross-section (CCS) data obtained from the drift times measured in the TWIM experiments (Tables S1−S4). CCS is the rotationally averaged forward-moving surface area of the complexes. The difference of CCSs of complexes **4**−**6** matches the different sizes of their respective cuboctahedron, octahedron, and *bis*triangle. These results were in accord with the averaged theoretical CCSs (2320.0 for **4**, 1598.6 for **5**, 816.7 for **6**), which were obtained by the trajectory method,[32−34] using the PA model that considers the collision process between ions and the buffer gas in the ion mobility region. The slight CCS differences between different charge states indicate that these complexes possess rigid and shape-persistent architectures.

Transmission electron microscopy (TEM) facilitated visualization of cuboctahedron cage **4**, octahedron **5**, and *bis*triangle **6**, directly revealing both the size and shape of individual molecules upon deposition of a dilute MeCN:DMF (2×10^{-6} M, 10:1, v/v) solution of the complexes with BPh_4^- counterions on carbon-coated grids (Cu, 400 mesh, Figure 4). At higher magnification, the images of single molecules exhibit sizes and shapes correlating with **4**−**6**.

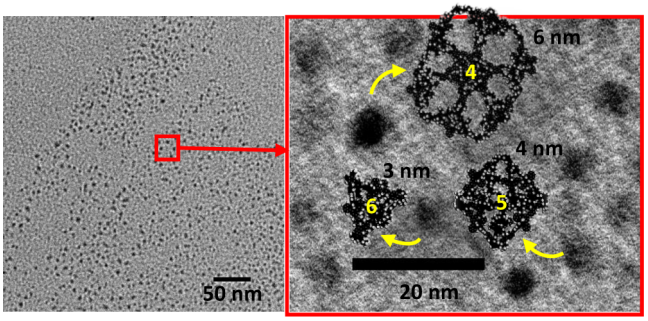

Figure 4. TEM images of a mixture of cages **4**−**6**. Lower magnification shows a uniform field of particles. Higher magnification shows a mixture of particle sizes and shapes roughly matching the structures.

The molecular modeling of **4**−**6** was performed. The modeling of the cuboctahedron **4** reveals a giant, cage-like structure of ca. 6.6 nm diameter. The 12 four-arm ligands with the flexible 18-crown ether centers and 24 metal ions were held together by pseudooctahedral ⟨tpy-Zn^{2+}-tpy⟩ linkages. Compared with the cuboctahedron cage (inner volume is 46 800 Å^3),[4] complex **4** shows larger overall size and volume 68 867 Å^3. The structure of **5** shows a highly symmetric octahedral cage, which has a 4.1 nm diameter and 9902 Å^3 volume. The modeling of **6** shows a sandwich-like cage, which has two triangular macrocycles connected with three flexible 18-crown-6 ethers. The longest distance between two oxygen atoms of the different crown ethers is 3.9 nm and the average distance between two triangular planes is 0.8 nm.

Preliminary investigation of potential guest binding properties was performed by the addition of small cations, such as K^+, Na^+, NH_4^+, to the larger complex **4**). ^{1}H NMR spectra exhibited a broadening (Figure S9) of the signals assigned to crown ether methylene moieties due to the crown−cation binding. The singlets of aryl groups adjacent to the crown ether units show a small, albeit noticeable, downfield shift when compared to the unbound specie. For example, similar crown ethers possessing associated Na^+ and K^+ show small 0.04 and 0.06 ppm downfield shifts. ESI-MS analysis also provided insight into the host−guest complexation of Na^+, K^+ or NH_4^+ ions with the crown ether units of sphere **4** (Figures S18−S21); encapsulated K^+ ion was observed to form the stronger association of these three ions. Finally, UV−vis absorption spectra of cage **6** and its corresponding Na^+, K^+, or NH_4^+ complexes reveal the expected similar λ_{max} peaks at ca. 285 and 340 nm.

In summary, the generation of semirigid, Archimedean-based, cuboctahedron and octahedron and a novel, superposed-*bis*triangle, using the new, designer, terpyridinyl monomer and transition metal ions (Zn^{2+}) is detailed. These structures show a dynamic equilibrium; altering the concentration, anions or solvents shifts the equilibrium. This confirms and expands the molecular fission−molecular fusion process and that this phenomenon is potentially applicable to other Archimedean structures and offers new entrée to molecular encapsulation. Incorporation of the 18-crown-6 moieties leads to conformationally adaptable building blocks and potential applications in cation recognition and catalytic activity.

DOI: 10.1021/jacs.6b07969
J. Am. Chem. Soc. 2016, 138, 12344−12347

■ ASSOCIATED CONTENT

Supporting Information

The Supporting Information is available free of charge on the ACS Publications website at DOI: 10.1021/jacs.6b07969.

Experimental procedures and characterization data including COSY and NOESY NMR, ESI- and TWIM-MS (PDF)

■ AUTHOR INFORMATION

Corresponding Authors

*G.R.N. newkome@uakron.edu.

*C.W. wesdemiotis@uakron.edu.

Notes

The authors declare no competing financial interest.

■ ACKNOWLEDGMENTS

The authors acknowledge funding from the National Science Foundation (CHE-1151991 GRN and CHE-1012636 CW).

■ REFERENCES

(1) Stagg, S. M.; LaPointe, P.; Razvi, A.; Gürkan, C.; Potter, C. S.; Carragher, B.; Balch, W. E. *Cell* **2008**, *134*, 474−484.

(2) Dill, K. A.; MacCallum, J. L. *Science* **2012**, *338*, 1042−1046.

(3) Pearse, B. M. F. *Proc. Natl. Acad. Sci. U. S. A.* **1976**, *73*, 1255−1259.

(4) Xie, T.-Z.; Guo, K.; Guo, Z.; Gao, W.-Y.; Wojtas, L.; Ning, G.-H.; Huang, M.; Lu, X.; Li, J.-Y.; Liao, S.-Y.; Chen, Y.-S.; Moorefield, C. N.; Saunders, M. J.; Cheng, S. Z. D.; Wesdemiotis, C.; Newkome, G. R. *Angew. Chem., Int. Ed.* **2015**, *54*, 9224−9229.

(5) Hua, Y.; Liu, Y.; Chen, C.-H.; Flood, A. H. *J. Am. Chem. Soc.* **2013**, *135*, 14401−14412.

(6) Pochorovski, I.; Ebert, M.-O.; Gisselbrecht, J.-P.; Boudon, C.; Schweizer, W. B.; Diederich, F. *J. Am. Chem. Soc.* **2012**, *134*, 14702−14705.

(7) Murakami, Y.; Hayashida, O. *Proc. Natl. Acad. Sci. U. S. A.* **1993**, *90*, 1140−1145.

(8) Samanta, D.; Mukherjee, P. S. *Chem. - Eur. J.* **2014**, *20*, 12483−12492. Han, M.; Engelhard, D. M.; Clever, G. H. *Chem. Soc. Rev.* **2014**, *43*, 1848−1860. Mosquera, J.; Ronson, T. K.; Nitschke, J. R. *J. Am. Chem. Soc.* **2016**, *138*, 1812−1815.

(9) Balzani, V.; Credi, A.; Venturi, M. *Proc. Natl. Acad. Sci. U. S. A.* **2002**, *99*, 4814−4817.

(10) Schweiger, M.; Seidel, S. R.; Arif, A. M.; Stang, P. J. *Inorg. Chem.* **2002**, *41*, 2556−2559. Ghosh, S.; Mukherjee, P. S. *Inorg. Chem.* **2009**, *48*, 2605−2613. Fujita, M.; Sasaki, O.; Mitsuhashi, T.; Fujita, T.; Yazaki, J.; Yamaguchi, K.; Ogura, K. *Chem. Commun.* **1996**, 1535−1536. Weilandt, T.; Troff, R. W.; Saxell, H.; Rissanen, K.; Schalley, C. A. *Inorg. Chem.* **2008**, *47*, 7588−7598. Carnes, M. E.; Collins, M. S.; Johnson, D. W. *Chem. Soc. Rev.* **2014**, *43*, 1825−1834.

(11) Chakrabarty, R.; Mukherjee, P. S.; Stang, P. J. *Chem. Rev.* **2011**, *111*, 6810−6918. McConnell, A. J.; Wood, C. S.; Neelakandan, P. P.; Nitschke, J. R. *Chem. Rev.* **2015**, *115*, 7729−7793. Cook, T. R.; Zheng, Y.-R.; Stang, P. J. *Chem. Rev.* **2013**, *113*, 734−777. Wang, M.; Wang, K.; Wang, C.; Huang, M.; Hao, X.-Q.; Shen, M.-Z.; Shi, G.-Q.; Zhang, Z.; Song, B.; Cisneros, A.; Song, M.-P.; Xu, B.; Li, X. *J. Am. Chem. Soc.* **2016**, *138*, 9258−9268. Fu, J.-H.; Lee, Y.-H.; He, Y.-J.; Chan, Y.-T. *Angew. Chem., Int. Ed.* **2015**, *54*, 6231−6235. Liu, D.; Jiang, Z.; Wang, M.; Yang, X.; Liu, H.; Chen, M.; Moorefield, C. N.; Newkome, G. R.; Li, X.; Wang, P. *Chem. Commun.* **2016**, *52*, 9773−9776. Constable, E. C.; Zhang, G.; Häussinger, D.; Housecroft, C. E.; Zampese, J. A. *J. Am. Chem. Soc.* **2011**, *133*, 10776−10779. Han, M.; Luo, Y.; Damaschke, B.; Gómez, L.; Ribas, X.; Jose, A.; Peretzki, P.; Seibt, M.; Clever, G. H. *Angew. Chem., Int. Ed.* **2016**, *55*, 445−449. *Functional Metallosupramolecular Materials*; Hardy, J. G.; Schacher, F. H., Eds.; Royal Society of Chemistry: Cambridge, 2015;. Wang, W.; Wang, Y.-X.; Yang, H.-B. *Chem. Soc. Rev.* **2016**, *45*, 2656−2693. Ludlow, J. M, III; Newkome, G. R. *Advances in Heterocyclic Chemistry*; Elsevier Publishing: Amsterdam, 2016, Chapter 8, pp 195−230.

(12) Caulder, D. L.; Brückner, C.; Powers, R. E.; Kõnig, S.; Parac, T. N.; Leary, J. A.; Raymond, K. N. *J. Am. Chem. Soc.* **2001**, *123*, 8923−8938.

(13) Kusukawa, T.; Fujita, M. *J. Am. Chem. Soc.* **2002**, *124*, 13576−13582.

(14) Sun, Q. F.; Iwasa, J.; Ogawa, D.; Ishido, Y.; Sato, S.; Ozeki, T.; Sei, Y.; Yamaguchi, K.; Fujita, M. *Science* **2010**, *328*, 1144−1147.

(15) Olenyuk, B.; Levin, M. D.; Whiteford, J. A.; Shield, J. E.; Stang, P. J. *J. Am. Chem. Soc.* **1999**, *121*, 10434−10435.

(16) Harris, K.; Fujita, D.; Fujita, M. *Chem. Commun.* **2013**, *49*, 6703−6712.

(17) Schultz, A.; Cao, Y.; Huang, M.; Cheng, S. Z. D.; Li, X.; Moorefield, C. N.; Wesdemiotis, C.; Newkome, G. R. *Dalton Trans.* **2012**, *41*, 11573−11575.

(18) Newkome, G. R.; Cho, T. J.; Moorefield, C. N.; Baker, G. R.; Saunders, M. J.; Cush, R.; Russo, P. S. *Angew. Chem., Int. Ed.* **1999**, *38*, 3717−3721.

(19) Newkome, G. R.; Wang, P.; Moorefield, C. N.; Cho, T. J.; Mohapatra, P.; Li, S.; Hwang, S.-H.; Lukoyanova, O.; Echegoyen, L.; Palagallo, J. A.; Iancu, V.; Hla, S.-W. *Science* **2006**, *312*, 1782−1785.

(20) Sarkar, R.; Guo, K.; Moorefield, C. N.; Saunders, M. J.; Wesdemiotis, C.; Newkome, G. R. *Angew. Chem., Int. Ed.* **2014**, *53*, 12182−12185.

(21) Wang, J.-L.; Li, X.; Lu, X.; Hsieh, I.-F.; Cao, Y.; Moorefield, C. N.; Wesdemiotis, C.; Cheng, S. Z. D.; Newkome, G. R. *J. Am. Chem. Soc.* **2011**, *133*, 11450−11453.

(22) Lu, X.; Li, X.; Cao, Y.; Schultz, A.; Wang, J.-L.; Moorefield, C. N.; Wesdemiotis, C.; Cheng, S. Z. D.; Newkome, G. R. *Angew. Chem., Int. Ed.* **2013**, *52*, 7728−7731.

(23) Superposed: "to lay (as a geometric figures, e.g. a triangle) upon another so as to make all parts coincide", www.MerrianWebster.com.

(24) Liu, Z.-Q.; Kubo, K.; Noro, S.-I.; Akutagawa, T.; Nakamura, T. *Cryst. Growth Des.* **2014**, *14*, 537−543.

(25) Kaller, M.; Staffeld, P.; Haug, R.; Frey, W.; Giesselmann, F.; Laschat, S. S. *Liq. Cryst.* **2011**, *38*, 531−553.

(26) Jarosz, P.; Lotito, K.; Schneider, J.; Kumaresan, D.; Schmehl, R.; Eisenberg, R. *Inorg. Chem.* **2009**, *48*, 2420−2428.

(27) Lu, X.; Li, X.; Guo, K.; Xie, T.-Z.; Moorefield, C. N.; Wesdemiotis, C.; Newkome, G. R. *J. Am. Chem. Soc.* **2014**, *136*, 18149−18155.

(28) Li, X.; Chan, Y.-T.; Newkome, G. R.; Wesdemiotis, C. *Anal. Chem.* **2011**, *83*, 1284−1290.

(29) Perera, S.; Li, X.; Soler, M.; Schultz, A.; Wesdemiotis, C.; Moorefield, C. N.; Newkome, G. R. *Angew. Chem., Int. Ed.* **2010**, *49*, 6539−6544.

(30) Hoaglund-Hyzer, C. S.; Counterman, A. E.; Clemmer, D. E. *Chem. Rev.* **1999**, *99*, 3037−3079.

(31) Brocker, E. R.; Anderson, S. E.; Northrop, B. H.; Stang, P. J.; Bowers, M. T. *J. Am. Chem. Soc.* **2010**, *132*, 13486−13494.

(32) Shvartsburg, A. A.; Jarrold, M. F. *Chem. Phys. Lett.* **1996**, *261*, 86−91.

(33) Jarrold, M. F. *Annu. Rev. Phys. Chem.* **2000**, *51*, 179−207.

(34) Shvartsburg, A.; Liu, B.; Siu, K. W. M.; Ho, K.-M. *J. Phys. Chem. A* **2000**, *104*, 6152−6163.

DOI: 10.1021/jacs.6b07969
J. Am. Chem. Soc. 2016, 138, 12344−12347